

# Anomalous Small-Angle X-ray Scattering Studies of Interlayer Heavy Metal Ions in Clay Minerals

Kathleen A. Carrado,\* P. Thiyagarajan,<sup>†</sup> Kang Song, and Randall E. Winans

Chemistry Division and Intense Pulsed Neutron Source Division, Argonne National Laboratory, 9700 S. Cass Avenue, Argonne, Illinois 60439

Received November 5, 1997. Revised Manuscript Received January 20, 1998

Anomalous small-angle X-ray scattering (ASAXS) has been exploited to monitor the solvation behavior of transition metal and lanthanide ions within the interlayers of the natural aluminosilicate clay mineral montmorillonite. The ASAXS technique can reveal the distribution of specific metallic species within a multicomponent and disordered matrix, which is typical of the semicrystalline smectite clays. The variations of scattering signal intensity as a function of absorption energy were monitored for Cu(II)–, Er(III)–, and Yb(III)–clays as a function of hydration. Two different hydration levels were probed: as prepared at ambient conditions, or so-called “dry” powders, and “wet” pastes. ASAXS intensities increase as the energy of the probing X-rays approaches the absorption energy of a given metal ion if it is associated with the interlayer solvent (water in this case) and decrease if the metal ion is associated with the solid matrix. The results show that (1) the ions are always associated with the clay in some fashion (they do not wash out into solution upon hydration, for example), (2) Cu(II) is well solvated within the interlayers of the clay, especially the wet sample, as expected, and (3) the lanthanide ions Er(III) and Yb(III) have associated with the clay interlayer surface, most likely as small hydrolyzed species even though the pH is well below the  $pK_h$  values. The latter ASAXS measurements provide the first direct evidence of this lanthanide hydrolysis phenomenon within clay interlayers, which has previously been inferred from elemental analysis and IR information.

## Introduction

Smectite clay minerals are layered metal silicates whose sheets can swell to incorporate up to several layers of water molecules. Each sheet is made up of one octahedral metal oxide layer, usually aluminum or magnesium, that is sandwiched by two tetrahedral silicate layers. Isomorphous substitutions within this framework give rise to a net negative charge on the lattice that is compensated for by the presence of exchangeable ions within the hydrated interlayer. Clays have a long history of applications as catalysts, catalyst supports, adsorbents, and ion exchangers.<sup>1</sup>

Clay minerals can incorporate heavy metal ions both within the lattice framework and between the interlayer regions. Our anomalous small-angle X-ray scattering (ASAXS) investigation into the former situation for a synthetic clay containing Ni(II) ions in the lattice has been published elsewhere.<sup>2</sup> For the latter case, clays ion-exchanged with various transition metal and lanthanide ions have now been examined at various hydration levels. The exchangeable interlayer metal ions impart a surface acidity on the clay that is variable depending upon the type of metal cation and the amount

of water present within the interlayer.<sup>1</sup> This surface acidity is vital to many hydroprocessing reactions of importance to catalytic petroleum refining, for example. In addition to catalytic applications, these experiments are also pertinent to the structure, diffusion, and reactivity of species involved in, for example, environmental remediation issues. A preliminary report of Er(III)–clay ASAXS<sup>2</sup> has now been expanded to include several different metal ions.

A description of both local and long-range atomic order associated with molecular assemblies in disordered media is essential for understanding the molecular basis for such issues as catalysis. Examples of such order include the structure and dynamics of molecular catalysts in solution and the distribution of solvent, solute, and counterions around catalytic surface sites. X-ray scattering provides a powerful tool for the measurement of long-range atomic order in globally disordered media. Disordered systems far more frequently describe materials used in the “real” world, yet they do not lend themselves to characterization by many of the standard techniques appropriate only for well-defined crystalline materials. The use of ASAXS to probe the atomic order of trace elements in condensed media is in its infancy because it is limited by the inherent weakness of the signals. To the best of our knowledge, this work represents the first foray into the use of ASAXS to probe a metal-oxide-based heterogeneous catalyst.

\* Author to whom all correspondence should be sent. Tel: (630) 252-7968. E-mail: kcarrado@anl.gov.

<sup>†</sup> Intense Pulsed Neutron Source Division.

(1) Grim, R. E. *Clay Mineralogy*, 2nd ed.; McGraw-Hill: New York, 1953.

(2) Thiyagarajan, P.; Carrado, K. A.; Wasserman, S. R.; Song, K.; Winans, R. E. *Rev. Sci. Instrum.* **1996**, *67* (9), 1.

**SAXS and ASAXS Methodology.** Small-angle X-ray scattering (SAXS) has numerous applications in chemistry, metallurgy, biology, polymer science, and colloidal systems. It examines correlations at distances from 10 to 1000 Å and provides information about the size, morphology, and interactions of a system of particles or pores in solution or in the solid state.<sup>3</sup> SAXS can also be used to follow the phase transitions, crystallization, and aggregation within a system. The SAXS intensity as a function of the momentum transfer is due to the distance correlations of all the atoms in the particles of interest. Anomalous SAXS (ASAXS) refers to extensions of standard SAXS experiments in which the energy of the probing X-rays are tuned near the absorption edge of an element in the sample. By performing SAXS experiments near the characteristic absorption edge of any given atom, it is possible to vary the contrast for scattering of that particular element. This systematic variation in contrast yields the partial scattering functions of the specific atomic species. In general, the atomic scattering can be expressed as

$$f(Q, E) = f_0(Q) + f'(Q, E) + i f''(Q, E) \quad (1)$$

where  $E$  is the energy of the probing X-rays and  $Q$  is the momentum transfer ( $Q = 4\pi \sin \theta/\lambda$ , where  $2\theta$  is the scattering angle and  $\lambda$  is the wavelength of X-rays). The parameters  $f'$  and  $f''$  are the real and imaginary parts of anomalous dispersion. They each vary sharply at energies within 10 eV of the absorption edge. The imaginary scattering factor,  $f''$ , represents the absorption of X-rays which results in photoemission of a core electron. Variation in  $f'$  is responsible for the change in contrast seen in ASAXS signals. These two quantities are related by the Kramers–Kronig relation. Typically  $f'$  is determined by measuring the energy-dependent absorption spectrum,  $f''$ , and applying the Kramers–Kronig transformation. Near the absorption edge of a given atom the scattering intensity,  $I$ , varies as a function of energy or wavelength (eq 2).

$$I(Q, \lambda) = I_n(Q) + f'(\lambda) I_C(Q, \lambda) + [f'^2(\lambda) + f''^2(\lambda)] I_R(Q) \quad (2)$$

Here  $I_n$  represents the nonresonant, energy-independent scattering. The cross term,  $I_C$ , reflects scattering between the specific element of interest and the remainder of the material, while  $I_R$  corresponds to the distance correlations of just the resonant scatterers.

Since  $f'$  and  $f''$  are sharply varying functions near the edge, these experiments require the highest possible energy resolution (of the order of  $\Delta\lambda/\lambda = 10^{-4}$ ) for the probing monochromatic X-rays. In these experiments we determine the small-angle scattering using incoming X-rays with four to five different energies. All but one of these energies are near the absorption edge of the atom of interest. The last measurement, using X-rays whose energy is 150 eV below the edge, gives a direct measurement of the nonresonant scattering,  $I_n$ , since at this energy  $f'$  and  $f''$  are quite small. From these sets of data, in principle one can obtain a set of three to four differential scattering data after the subtraction

of  $I_n$ . If the SAXS data as a function of energy are placed on an absolute scale, one can then use  $f'$  and  $f''$  values to obtain the partial structure factors,  $I_C$  and  $I_R$ , by least-squares analysis. The maximum variation in the SAXS signals near the edge depends on the maximum value of the variation of  $f'$  for a given atom. In general, the variation of  $f'$  is larger near the  $L_{III}$  edges of lanthanides than for the K edges of transition metals. We have, however, successfully monitored both types of metals at comparable weight loadings.

ASAXS is a fairly new technique, first reported in 1985 for condensed media with the analysis of metal alloys<sup>4f</sup> and somewhat earlier for solution-phase biochemical systems.<sup>5</sup> While alloys remain the focus of most ASAXS investigations,<sup>4</sup> other systems that have proven amenable to such analysis are metallic glasses,<sup>6</sup> ionomers,<sup>7</sup> and metal oxide gels.<sup>8</sup> Some review articles are available with general background information for the interested reader.<sup>9,10</sup> Only a few references exist where ASAXS has been exploited to characterize heterogeneous catalysts or supports, including our previous work<sup>2</sup> and a study of Pt/C electrocatalysts.<sup>11</sup>

## Experimental Section

Bentolite L, a natural  $Ca^{2+}$ -bentonite that has been purified to remove all but 0.2 wt % Fe impurities, was obtained from Southern Clay Products. This was ion-exchanged with Cu(II), Er(III), and Yb(III) ions by stirring 1 g of clay in 100 mL of 0.1 M solutions of the hydrated chloride salts overnight, followed by centrifugation, washing, and drying at room temperature. X-ray powder diffraction patterns were obtained on a Scintag PAD V instrument with Cu K $\alpha$  radiation.

The powder and thick slurry samples were contained in a cell with Kapton windows for SAXS measurements. The samples were measured at SAXS beamline BL 4-2 at the Stanford Synchrotron Radiation Laboratory in Stanford, CA. This beamline has a platinum-coated mirror which focuses the X-rays in the horizontal direction. A 62  $\mu$ rad slit upstream from this mirror defines the energy resolution of the probing X-rays at <2 eV. The reflected beam from the mirror is monochromated by a double-crystal Si(111) monochromator. The cross-sectional area of the X-ray beam, 3 mm  $\times$  1 mm, is defined by two slits. The beam was focused at a 20 cm long one-dimensional position-sensitive gas detector placed in the vertical direction. The sample was located approximately 2.2 m upstream to the detector. Two ionization chambers, one before and one after the sample, monitored the intensity of the incident and absorbed X-rays. These monitors were also used to determine the absorption edge for the metal of interest

(4) (a) Simon, J. P. *Ann. Phys. (Paris)* **1995**, *20*, C3/127–134. (b) Bajguirani, H. R. *Nanostruct. Mater.* **1994**, *4*, 833–50. (c) Regan, M. J. *Mater. Res. Soc. Symp. Proc.* **1993**, *307*, 347–32. (d) Lyon, O.; Simon, J. P. *J. Phys. F: Met. Phys.* **1988**, *18*, 1787–99. (e) Goudeau, P.; Naudon, A.; Chamberod, A.; Rodmacq, B.; Williams, C. E. *Europhys. Lett.* **1987**, *3*, 269–75. (f) Lyon, O. *J. Appl. Crystallogr.* **1985**, *18*, 480.

(5) (a) Miake-Lye, R. C.; Doniach, S.; Hodgson, K. O. *Biophys. J.* **1983**, *41*, 287. (b) Stuhmann, H. B.; Notbohm, H. *Proc. Natl. Acad. Sci. U.S.A.* **1981**, *78*, 6216.

(6) (a) Brueckner, R. *Nucl. Instrum. Methods Phys. Res., Sect. B* **1995**, *97*, 190. (b) Goerigk, G. *J. Appl. Crystallogr.* **1994**, *27*, 907.

(7) (a) Chu, B. *Ionomers* **1996**, *35*. (b) Chu, B. *Macromolecules* **1993**, *26*, 994. (c) Chu, B. *Mater. Res. Soc. Symp. Proc.* **1990**, *171* (*Polym. Based Mol. Compos.*), 237.

(8) Gerber, T. *J. Phys. IV* **1993**, *3*(C8), 385.

(9) (a) Naudon, A. *NATO ASI Ser., Ser. C* **1995**, *451*, 203. (b) Simon, J. P.; Lyon, O. In *Resonance Anomalous X-ray Scattering*; Materlik, G., Sparks, C. J., Fischer, K., Eds.; North-Holland: Amsterdam, 1994, 305–322.

(10) Epperson, J. E.; Thiyagarajan, P. *J. App. Cryst.* **1988**, *21*, 652–662 and references therein.

(11) Haubold, H.-G.; Wang, X. H.; Jungbluth, H.; Goerigk, G.; Schilling, W. *J. Mol. Struct.* **1996**, *383*, 283.

(3) Glatter, O.; Kratky, O. In *Small Angle X-ray Scattering*; Academic Press: New York, 1982.

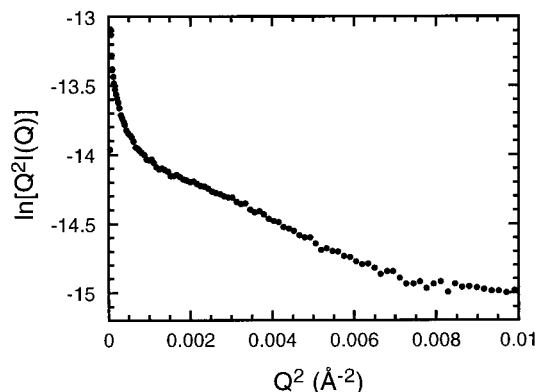


**Figure 1.** Modified Guinier sheet analysis of the SAXS data for Cu(II)-clay as the "dry" powder, taken well away from the copper absorption edge at 8782 eV. Error bars are of equal or lesser size than the data points and so were omitted for clarity.

in each of the samples. The entire beam path was under vacuum except at the sample. In this configuration the SAXS instrument can measure data in the  $Q$  region from 0.008 to  $0.25 \text{ \AA}^{-1}$ .

The acquisition time for each scattering profile was 5 min. During the acquisition of the scattering data, the energy of the incoming X-rays was cycled through each of the energies for 5–10 cycles, depending on the desired statistical precision. This procedure aided in the assessment of the stability of the sample as well as the position of the X-ray beam. Using metal foils, an absorption edge at 8359.2 eV corresponding to the  $L_{III}$  edge of Er was found (actual value is 8358 eV). The ASAXS for the powder samples was then measured at 8153, 8323, 8338, 8346, and 8353 eV. Similar procedures were used for the remaining metal ions at their respective absorption energy edges (Cu K and Yb  $L_{III}$  edges at 8979 and 8944 eV, respectively).

## Results and Discussion

The dry and wet samples were analyzed by ASAXS and X-ray powder diffraction (XRD). XRD revealed that the interlayer spacings for all metal-clays increased by 4–7 Å upon hydration (formation of a wet paste) to 19.5–20 Å. This indicates that the interlayer has accommodated more water layers. Typically they expand from one or two layers of water to three layers.<sup>1</sup> The issue of interest here is to monitor the hydration of the metal ion during this process to better understand its relative mobility. Modified Guinier analysis of the ASAXS data was used to extract the correlations for the sheetlike clay particles. This approach is based on the fact that the intensity of scattering for infinitely large sheets varies as  $Q^{-2}$ .<sup>3</sup> When a modified Guinier analysis is performed in the low- $Q$  region by plotting  $\ln[Q^2 I(Q)]$  as a function of  $Q^2$ , a linear region indicates the presence of sheetlike particles. Figure 1 displays the full low- $Q$  data range ( $Q^2 = 0\text{--}0.01 \text{ \AA}^{-2}$ ) for Cu(II)-clay, showing clearly the existence of a linear region from 0.001 to  $0.008 \text{ \AA}^{-2}$ . This verifies that we are in fact measuring the scattering of the clay sheets. One set of scattering data, that taken at 8782 eV, is shown in this figure, which is well away from the copper absorption edge. Figures 2 and 3 display the modified Guinier sheet analyses of the scattering for the Cu(II)- and Yb(III)-clay systems, respectively. Results for Er(III)-clay were similar to those for Yb(III)-clay. Scattering data taken at all of the measured energies for each system is presented in these latter plots (with

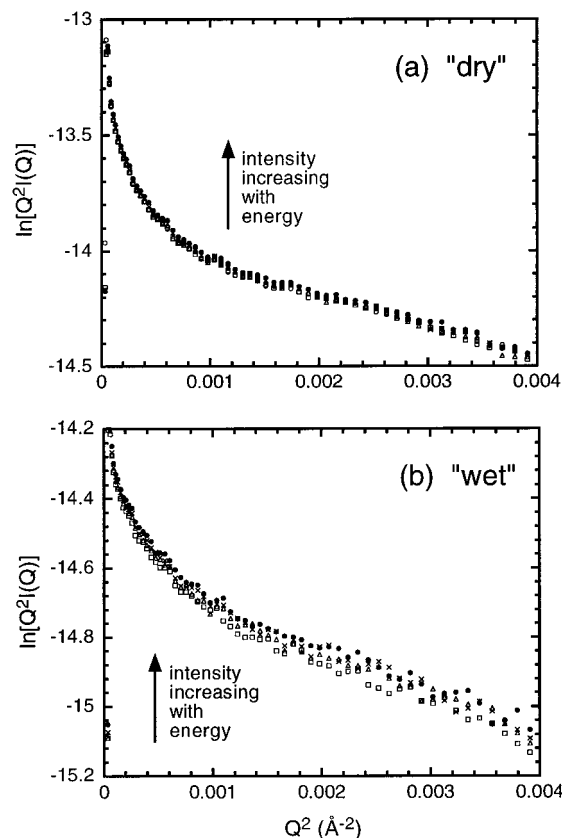


**Figure 2.** Modified Guinier sheet analysis of the ASAXS data for Cu(II)-clay as (a) the "dry" powder and (b) the "wet" paste. Error bars are of equal or lesser size than the data points and so were omitted for clarity. Scattering was measured at absorption energies:<sup>12</sup> (○) 8782, (□) 8946, (△) 8961, (×) 8969, and (●) 8975 eV.

one exception<sup>12</sup>), with  $Q^2$  plotted from 0 to  $0.004 \text{ \AA}^{-2}$ .

A modified Guinier plot of several SAXS measurements systematically taken at various energies approaching a metal's absorption edge will reveal the ASAXS effect if that metal is indeed associated with the matrix of choice. The ASAXS effect manifests itself in a systematic change in intensity with the change in energy. Since our modified Guinier analysis is chosen to analyze sheetlike particles, a systematic variation in scattering intensity with absorption energy in such a plot unequivocally reveals that the metal must be associated with the two-dimensional, platelet, clay matrix. Further, ASAXS intensities should increase with absorption energy if the metal ion is associated with the interlayer solvent (water, in this case) and decrease if the metal ion is associated with the solid matrix.<sup>2</sup>

The following discussion is provided to explain these various intensity changes. The scattering cross section of a given system is determined by the atomic scattering factor of the constituent atoms. The scattering factor includes the three terms presented in eq 1. Near the characteristic absorption edge,  $f'$  has a minimum. Let us consider the system of dispersed clay particles in water. The scattering from this system is determined by the number density of the particles, the square of

(12) Note that the data collected for the wet sample of Cu-clay at 8782 eV is not presented but that the trend of increasing intensity with increasing energy is still clearly evident.

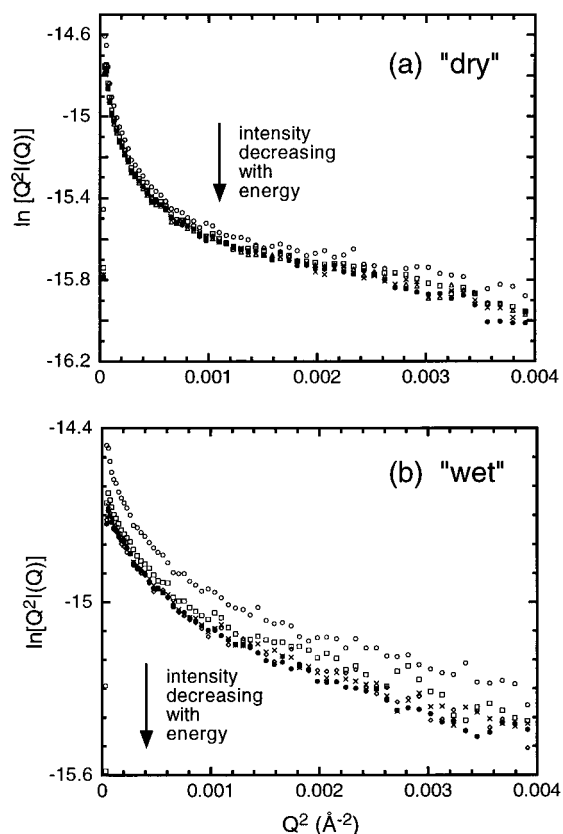


**Figure 3.** Modified Guinier sheet analysis of the ASAXS data for Yb(III)-clay as (a) the "dry" powder and (b) the "wet" paste. Error bars are of equal or lesser size than the data points and so were omitted for clarity. Scattering was measured at absorption energies: (○) 8744, (□) 8904, (△) 8919, (×) 8931, and (●) 8938 eV.

the volume of the particles, and the square of the difference in the electron densities of the particles and water. Note that the electron density of clays will always be higher than that of water. In this scenario, if the labels of interest are located within the clay lattice itself (e.g., Ni-SMM clay<sup>2</sup>), the difference in the electron density between the clay and the water will decrease as one approaches the absorption edge of a given metal atom. This is because the net  $f'$  value will decrease while that of the H<sub>2</sub>O remains the same. That means that the electron density difference decreases as the energy of the probing X-rays approaches the edge, and thus the scattering intensity should monotonically decrease with increasing energy.<sup>6</sup>

On the other hand, if the metal atoms are associated with the solvent but not with the clays, then  $f'$  of the clay remains the same but that of the solvent decreases. This means that the net electron density difference increases as one approaches the absorption edge. This will result in a monotonic increase in the scattering intensity with increasing energy as the energy of the probing X-rays approaches the absorption edge of a given atom.<sup>10</sup> For the same concentration of the metal atoms, the above effect will be much larger for the former case (ion-clay interaction) than that for the latter (ion-solvent interaction). This is because the signal intensity that is due to constructive interference from the scattering waves from the labels in clays is completely lost from similar atoms in solution.

**Table 1. Hydrolysis Study**

ion-clay	pH during ion exchange	$pK_h^a$
Cu(II)	4.5	7.6
Er(III)	5.5	8.7
Yb(III)	5.5	8.0

<sup>a</sup> Negative log of the hydrolysis constant.<sup>13</sup>

Although there is a very slight ASAXS effect observed in the dry samples (Figures 2a and 3a), especially for the Cu(II)-clay, the margin of error precludes us from deducing where the ions might reside. Much more of an effect is observed for the wet samples. On the basis of the XRD results of increased basal spacings with addition of water, we were expecting in all cases to see that the ions would be associated with the solvent (water) in the slurries. This did occur for the Cu-clay, corroborating our results from a local-environment, short-range order study by X-ray absorption spectroscopy.<sup>13</sup> However, neither of the lanthanide-clays showed an ion-solvent interaction upon increased hydration. The layer-layer correlations of the  $\ln Q^2 I(Q)$  vs  $Q^2$  plots clearly indicate that the lanthanide ions do remain associated with the clay, proving that they are ion-exchanged and not simply precipitated out as a separate hydroxide phase on the surface, for instance. But the decrease in scattering intensity with absorption energy indicates that these lanthanide ions apparently are not fully solvated within the interlayer. This latter result was not expected and it is postulated that these ions are instead associated as hydrolyzed species with the clay surface.

The pH of each metal ion-clay slurry during ion exchange was monitored, and were well below the hydrolysis constants of the respective ion in every case (see Table 1). At pH's above the  $pK_h$  values,<sup>14</sup> Pb(II) and Cr(III) will form oxide-hydroxide precipitates on clay surfaces.<sup>15</sup> Below this critical pH, these ions simply exist as exchangeable cations within the interlayer. Cu(II) also behaves in this manner because the exchange takes place well below its  $pK_h$ .

Lanthanide ions appear to behave somewhat differently, however. Several years ago, a suite of articles reported how lanthanide sorption by montmorillonite was effected by pH, concentration, temperature, and pressure.<sup>16</sup> One finding reported that lanthanide hydrolysis occurs at lower pH values than are observed for aqueous solutions in the absence of clay.<sup>16c</sup> The presence of montmorillonite modifies the pH value at which the hydrolysis occurs, and "precipitation" commences at a lower value. This value was determined to be  $>5$ , which is in fact the case for our materials (pH 5.5). Hydrolysis is halted when the pH of the medium is acidified to  $<5$ . Er(III) and Yb(III) have similar ionic radii at 1.14 and 1.12 nm, respectively (coordination

(13) Carrado, K. A.; Wasserman, S. R. *J. Am. Chem. Soc.* **1993**, *115*, 3394.

(14) (a) Baes, C. F.; Mesmer, R. E. *The Hydrolysis of Cations*; Wiley & Sons: New York, 1976. (b) Huheey, J. E. *Inorganic Chemistry*; Harper & Row: New York, 1978; p 266.

(15) Gan, H.; Bailey, G. W.; Yu, Y. S. *Clays Clay Miner.* **1996**, *44*, 734.

(16) (a) Miller, S. E.; Heath, G. H.; Gonzalez, R. D. *Clays Clay Miner.* **1983**, *31*, 17. (b) Miller, S. E.; Heath, G. H.; Gonzalez, R. D. *Clays Clay Miner.* **1982**, *30*, 111. (c) Bruque, S.; Mozas, T.; Rodriguez, A. *Clay Miner.* **1980**, *15*, 413. (d) Bruque, S.; Mozas, T.; Rodriguez, A. *Clay Miner.* **1980**, *15*, 421.

number 8).<sup>14b</sup> Therefore, they likely have similar hydration energies and are expected to behave the same within the clay interlayer environment. It has been proposed that the specialized, localized electrostatic environment within a clay interlayer is strong enough to dissociate water ligands about a lanthanide ion, releasing OH<sup>-</sup> ions which then react to form hydroxides.<sup>16c</sup>

The clay surface may have an even more active role, however. With large basal spacings (ca. 20 Å), hydrated ions experience an equipotential clay surface and can interact with the clay either through hydrogen bonding (complete hydration sphere) or direct residence on the interlayer surface (partial hydration sphere).<sup>16b</sup> This latter state has been the one proposed for clay suspensions and pastes. In this case, hydrolysis involves dissociation of a coordinated water molecule followed by fixation of the metal ion to the clay. Sites available for this complexation are (1) the hexagonal holes created by the basal silicate surface and (2) other surface oxygen atoms. Both of these sites have been proposed to account for an adsorption of lanthanide ions in excess of that predicted by the cation-exchange capacity.<sup>16b</sup> Our ASAXS results appear to support the view that the ions have indeed bonded to the silicate itself, rather than simply precipitate out separately as oxide-hydroxide phases on the surface. The scattering data for this study were not collected on an absolute scale, which precludes the use of known variables in the Kramers-Kronig equation. A more careful study is now underway to obtain scattering data on an absolute scale. This will provide the data necessary for quantification of the  $I_R$  and  $I_C$  distance correlations. Ion exchanges at lower pH values are also planned to deter hydrolysis in the lanthanide-clay samples.

## Conclusions

We have demonstrated that the ASAXS effect can be observed in aluminosilicate clays containing 2–3 wt % transition metal and lanthanide ions. Further, this effect can be used to elucidate how the ions solvate when the clay is hydrated to form suspensions or pastes. For instance, Cu(II) solvates within the interlayer and therefore behaves as a mobile species capable of facile ion exchange. At certain conditions, ASAXS shows that some lanthanides (at least the smaller Er(III) and Yb(III) ions) will behave in an opposite manner and instead bind to the clay lattice. A thorough understanding of the kinetics and mechanisms of heavy metal ion sorption on clay mineral surfaces is a critical issue and the subject of recent intensive study.<sup>17</sup> These results contribute to the view of metal ion interactions at the clay-water interface.

**Acknowledgment.** This work was performed under the auspices of the U.S. Department of Energy, Office of Basic Energy Sciences, Divisions of Chemical Sciences and Materials Sciences, under contract no. W-31-109-ENG-38. Research at SSRL is supported by the Department of Energy, Office of Basic Energy Sciences. We thank H. Tsuruta for assistance with BL-4-2 at SSRL and L. Xu (ANL) for performing XRD measurements.

CM970723Q

---

(17) (a) Stumm, W. *Chemistry of the Solid-Water Interface*, Wiley-Interscience: New York, 1992. (b) Scheidegger, A. M.; Lample, G. M.; Sparks, D. L. *J. Coll. Interface Sci.* **1997**, *186*, 118.